

# Modified triplet-wave expansion method applied to the alternating Heisenberg chain

A. Collins, C. J. Hamer, and Zheng Weihong

*School of Physics, The University of New South Wales, Sydney, NSW 2052, Australia*

(Received 1 June 2006; published 19 October 2006)

An alternative triplet-wave expansion formalism for dimerized spin systems is presented, a modification of the “bond operator” formalism of Sachdev and Bhatt. Projection operators are used to confine the system to the physical subspace, rather than constraint equations. The method is illustrated for the case of the alternating Heisenberg chain, and comparisons are made with the results of dimer series expansions and exact diagonalization. Some discussion is included of the phenomenon of “quasiparticle breakdown” as it applies to the two-triplon bound states in this model.

DOI: [10.1103/PhysRevB.74.144414](https://doi.org/10.1103/PhysRevB.74.144414)

PACS number(s): 75.10.Jm, 05.30.-d, 75.30.Kz

## I. INTRODUCTION

There has been much interest recently in the phenomenon of *dimerization* in  $S=1/2$  Heisenberg antiferromagnets, where pairs of neighboring spins couple to form  $S=0$  singlet dimers. The dimerization may arise due to inhomogeneous bond interactions, as in the alternating Heisenberg chain (AHC) model, or the Shastry-Sutherland model in two dimensions.<sup>1</sup> Alternatively, it may emerge spontaneously, as the result of frustration:<sup>2</sup> this seems to occur in the  $J_1$ - $J_2$  square lattice model at intermediate coupling values, for instance, although there is disagreement as to whether the pattern of dimerization is ordered (“valence bond solid”)<sup>3,4</sup> or disordered (“valence bond liquid” or “resonating valence bond”).<sup>5,6</sup>

To understand the properties of dimerized phases, it is useful to construct an appropriate lattice formalism describing the dimers and their spin-triplet excitations. The physics of the system can then be connected with the properties of the elementary triplet excitations; and one can also use the formalism to construct a continuum “effective Lagrangian” field theory for the system at hand. Such a formalism was the “bond-operator” representation constructed by Sachdev and Bhatt<sup>7</sup> (see also Chubukov<sup>8</sup>) some years ago, which is analogous to the spin-wave representation traditionally used to describe the magnetically ordered phases of these systems.<sup>9</sup>

Sachdev and Bhatt<sup>7</sup> considered two spins  $\mathbf{S}_1$  and  $\mathbf{S}_2$  at either end of a single bond on the lattice, forming a dimer. They introduced a singlet and three triplet boson creation operators to form the corresponding states from the vacuum:

$$\begin{aligned} |s\rangle &= s^\dagger|0\rangle = \frac{1}{\sqrt{2}}(|\uparrow\downarrow\rangle - |\downarrow\uparrow\rangle), \\ |t_x\rangle &= t_x^\dagger|0\rangle = -\frac{1}{\sqrt{2}}(|\uparrow\uparrow\rangle - |\downarrow\downarrow\rangle), \\ |t_y\rangle &= t_y^\dagger|0\rangle = \frac{i}{\sqrt{2}}(|\uparrow\uparrow\rangle + |\downarrow\downarrow\rangle), \\ |t_z\rangle &= t_z^\dagger|0\rangle = \frac{1}{\sqrt{2}}(|\uparrow\downarrow\rangle + |\downarrow\uparrow\rangle). \end{aligned} \quad (1)$$

Then the spin operators can be represented

$$S_{1\alpha} = \frac{1}{2}[s^\dagger t_\alpha + t_\alpha^\dagger s - i\epsilon_{\alpha\beta\gamma} t_\beta^\dagger t_\gamma],$$

$$S_{2\alpha} = \frac{1}{2}[-s^\dagger t_\alpha - t_\alpha^\dagger s - i\epsilon_{\alpha\beta\gamma} t_\beta^\dagger t_\gamma] \quad (2)$$

(where  $\alpha, \beta, \gamma$  take values  $x, y,$  or  $z$ ), with the constraint that physical states must satisfy

$$s^\dagger s + t_\alpha^\dagger t_\alpha = 1. \quad (3)$$

They applied this formalism to develop a mean field theory of the frustrated square-lattice antiferromagnet.

The problem with this approach is that the constraint (3) is awkward to implement analytically. Kotov *et al.*<sup>10</sup> have applied an alternative “Brueckner approach,” in which the singlet operator is discarded, leaving only the constraint that two triplet excitations are not allowed on the same site (bond). This is implemented by an infinite on-site repulsion term between triplets, which is applied using an analytic Brueckner approach, valid when the density of triplets is small. The approach has been applied to the two-layer Heisenberg model,<sup>10,11</sup> the quantum spin-ladder,<sup>12,13</sup> and the dimerized Heisenberg chain with frustration,<sup>14</sup> and some useful physical insights have been obtained. In particular, the occurrence of two-particle bound states formed from the elementary triplet excitations seems to be generic in these models. Nevertheless, the Brueckner implementation of the on-site repulsion term is also somewhat awkward to apply and difficult to carry through in higher orders.

Here we present an alternative approach in which the triplet exclusion constraint is implemented automatically by means of projection operators. We also use a “modified” formalism, analogous to modified spin-wave theory,<sup>15,16</sup> in which the two-body terms in the Hamiltonian are diagonalized through to the highest order calculated. The absence of any constraint makes the formalism easier and more transparent to apply. The only drawback is the appearance of extra many-body interaction terms in the Hamiltonian, so that carrying the calculation to high orders would require the aid of a computer.

To illustrate the formalism, we apply it to the case of the alternating Heisenberg chain (AHC). This model has itself attracted much attention recently, as new materials such as

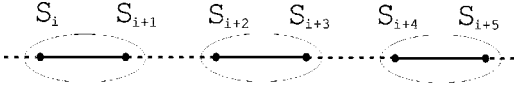


FIG. 1. The alternating Heisenberg chain.

$\text{Cu}(\text{NO}_3)_2 \cdot 2.5\text{D}_2\text{O}$  (Refs. 17 and 18) have been constructed which appear to conform to this simple model, while at the same time more powerful neutron scattering facilities are coming on-line to explore their properties. For a review and further references, see Barnes *et al.*<sup>19</sup> On the theoretical side, Uhrig and Schulz<sup>20</sup> used a field theory approach to predict the appearance of both singlet ( $S=0$ ) and triplet ( $S=1$ ) bound states below the two-triplet continuum. This was confirmed by later studies.<sup>14,21,22</sup> Bouzerar and Sil<sup>23</sup> and Shevchenko *et al.*<sup>14</sup> have treated the AHC using the Brueckner approach; while Singh and Zheng,<sup>24</sup> Trebst *et al.*,<sup>25</sup> and Zheng *et al.*<sup>26</sup> have carried out high-order dimer series expansions for the model, which give an accurate numerical picture of the dimerized phase.

In Sec. II, we lay out the triplet-wave expansion formalism for the case of the alternating chain. In Sec. III, the expansion to leading orders on powers of the coupling  $\lambda$  is discussed for the ground state energy and energy gap. In Sec. IV, numerical results are presented for the ground-state energy, the one-particle spectrum, the two-triplon bound states, and the exclusive structure factors for these states. A summary and conclusions are presented in Sec. V.

## II. TRIPLET-WAVE EXPANSION

The Hamiltonian for the alternating Heisenberg chain can be written

$$H = \sum_{i \text{ odd}} \mathbf{S}_i \cdot \mathbf{S}_{i+1} + \lambda \sum_{i \text{ even}} \mathbf{S}_i \cdot \mathbf{S}_{i+1}. \quad (4)$$

For  $\lambda=0$ , the system reduces to independent dimers as shown in Fig. 1. Let us consider a single dimer with two spins  $\mathbf{S}_1, \mathbf{S}_2$ . The four states in the Hilbert space consist of a singlet and three triplet states with total spin  $S=0, 1$ , respectively, and eigenvalues

$$\mathbf{S}_1 \cdot \mathbf{S}_2 = \begin{cases} -3/4 & (S=0) \\ +1/4 & (S=1) \end{cases}. \quad (5)$$

We denote the singlet ground state as  $|0\rangle$ , and introduce triplet creation operators that create the triplet states out of the vacuum  $|0\rangle$ , as follows:

$$\begin{aligned} |0\rangle &= \frac{1}{\sqrt{2}}[|\uparrow\downarrow\rangle - |\downarrow\uparrow\rangle], \\ |1,x\rangle &= t_x^\dagger|0\rangle = -\frac{1}{\sqrt{2}}[|\uparrow\uparrow\rangle - |\downarrow\downarrow\rangle], \\ |1,y\rangle &= t_y^\dagger|0\rangle = \frac{i}{\sqrt{2}}[|\uparrow\uparrow\rangle + |\downarrow\downarrow\rangle], \end{aligned}$$

$$|1,z\rangle = t_z^\dagger|0\rangle = \frac{1}{\sqrt{2}}[|\uparrow\downarrow\rangle + |\downarrow\uparrow\rangle]. \quad (6)$$

Then the spin operators  $\mathbf{S}_1$  and  $\mathbf{S}_2$  can be represented in terms of triplet operators by

$$\begin{aligned} S_{1\alpha} &= \frac{1}{2}[t_\alpha^\dagger(1 - t_\gamma^\dagger t_\gamma) + (1 - t_\gamma^\dagger t_\gamma)t_\alpha - i\epsilon_{\alpha\beta\gamma}t_\beta^\dagger t_\gamma], \\ S_{2\alpha} &= \frac{1}{2}[-t_\alpha^\dagger(1 - t_\gamma^\dagger t_\gamma) - (1 - t_\gamma^\dagger t_\gamma)t_\alpha - i\epsilon_{\alpha\beta\gamma}t_\beta^\dagger t_\gamma], \end{aligned} \quad (7)$$

where  $\alpha, \beta, \gamma$  take the values  $x, y, z$  and repeated indices are summed over. This is similar to the representation of Sachdev and Bhatt,<sup>7</sup> except that we have omitted singlet operators  $s^\dagger, s$ , but used projection operators  $(1 - t_\gamma^\dagger t_\gamma)$  instead. Assume the triplet operators obey bosonic commutation relations

$$[t_\alpha, t_\beta^\dagger] = \delta_{\alpha\beta}, \quad (8)$$

then one can show that within the physical subspace (i.e., total number of triplet states is 0 or 1), the representation (7) obeys the correct spin operator algebra

$$[S_{1\alpha}, S_{1\beta}] = i\epsilon_{\alpha\beta\gamma}S_{1\gamma}, \quad [S_{2\alpha}, S_{2\beta}] = i\epsilon_{\alpha\beta\gamma}S_{2\gamma}, \quad (9)$$

$$[S_{1\alpha}, S_{2\beta}] = 0, \quad (10)$$

$$\mathbf{S}_1^2 = \mathbf{S}_2^2 = 3/4, \quad \mathbf{S}_1 \cdot \mathbf{S}_2 = t_\alpha^\dagger t_\alpha - 3/4. \quad (11)$$

The projection operators ensure that we remain within the subspace.

Returning to the alternating chain, we can now define triplet operators  $t_{n\alpha}^\dagger, t_{n\alpha}$  for each dimer  $n$  along the chain. For a chain of  $N$  dimers, the Hamiltonian now can be expressed in terms of triplet operators as

$$\begin{aligned} H &= -\frac{3N}{4} + \sum_n t_{n\alpha}^\dagger t_{n\alpha} - \frac{\lambda}{4} \sum_n \{t_{n\alpha}^\dagger(1 - t_{n\gamma}^\dagger t_{n\gamma})t_{n+1,\alpha}^\dagger \\ &\quad \times (1 - t_{n+1,\delta}^\dagger t_{n+1,\delta}) + (1 - t_{n\gamma}^\dagger t_{n\gamma})t_{n\alpha}(1 - t_{n+1,\delta}^\dagger t_{n+1,\delta})t_{n+1,\alpha} \\ &\quad + t_{n\alpha}^\dagger(1 - t_{n\gamma}^\dagger t_{n\gamma})(1 - t_{n+1,\delta}^\dagger t_{n+1,\delta})t_{n+1,\alpha} \\ &\quad + (1 - t_{n\gamma}^\dagger t_{n\gamma})t_{n\alpha}t_{n+1,\alpha}^\dagger(1 - t_{n+1,\delta}^\dagger t_{n+1,\delta})\} \\ &\quad + \frac{\lambda}{4} \sum_n t_{n\beta}^\dagger t_{n\gamma}(t_{n+1,\gamma}^\dagger t_{n+1,\beta} - t_{n+1,\beta}^\dagger t_{n+1,\gamma}) \\ &\quad + i\frac{\lambda}{4}\epsilon_{\alpha\beta\gamma} \sum_n \{t_{n\alpha}^\dagger(1 - t_{n\delta}^\dagger t_{n\delta})t_{n+1,\beta}^\dagger t_{n+1,\gamma} \\ &\quad - t_{n\beta}^\dagger t_{n\gamma}t_{n+1,\alpha}^\dagger(1 - t_{n+1,\delta}^\dagger t_{n+1,\delta}) \\ &\quad + (1 - t_{n\delta}^\dagger t_{n\delta})t_{n\alpha}t_{n+1,\beta}^\dagger t_{n+1,\gamma} \\ &\quad - t_{n\beta}^\dagger t_{n\gamma}(1 - t_{n+1,\delta}^\dagger t_{n+1,\delta})t_{n+1,\alpha}\}. \end{aligned} \quad (12)$$

This expression includes terms containing up to six triplet operators. For the purposes of the present calculations, we shall drop terms with more than four triplet operators henceforward.

Next, perform a Fourier transform

$$t_{k\alpha} = \left(\frac{1}{N}\right)^{1/2} \sum_n e^{ikn} t_{n\alpha},$$

$$t_{k\alpha}^\dagger = \left(\frac{1}{N}\right)^{1/2} \sum_n e^{-ikn} t_{n\alpha}^\dagger \quad (13)$$

(we set the spacing between dimers  $d=1$ ), then the Hamiltonian becomes

$$H = -\frac{3N}{4} + \sum_k t_{k\alpha}^\dagger t_{k\alpha} - \frac{\lambda}{4} \sum_k \cos k [t_{k\alpha}^\dagger t_{-k\alpha}^\dagger + t_{k\alpha} t_{-k\alpha} + 2t_{k\alpha}^\dagger t_{k\alpha}]$$

$$+ \frac{\lambda}{2\sqrt{N}} \epsilon_{\alpha\beta\gamma} \sum_{123} \delta_{1+2-3} \sin k_1 [t_{1\alpha}^\dagger t_{2\beta}^\dagger t_{3\gamma}^\dagger + t_{3\gamma}^\dagger t_{1\alpha}^\dagger t_{2\beta}^\dagger]$$

$$+ \frac{\lambda}{2N} \sum_{1234} \{\delta_{1+2+3-4} t_{1\alpha}^\dagger t_{2\alpha}^\dagger t_{3\gamma}^\dagger t_{4\gamma} \cos k_1$$

$$+ \delta_{1-2-3-4} t_{1\gamma}^\dagger t_{2\gamma}^\dagger t_{3\alpha}^\dagger t_{4\alpha} \cos k_4$$

$$+ \delta_{1+2-3-4} [t_{1\alpha}^\dagger t_{2\gamma}^\dagger t_{3\gamma}^\dagger t_{4\alpha} \cos k_4 + t_{1\alpha}^\dagger t_{2\gamma}^\dagger t_{3\gamma}^\dagger t_{4\alpha} \cos k_1]\}$$

$$+ \frac{\lambda}{4N} \sum_{1234} \delta_{1+2-3-4} [t_{1\gamma}^\dagger t_{2\beta}^\dagger t_{3\beta}^\dagger t_{4\gamma} - t_{1\beta}^\dagger t_{2\beta}^\dagger t_{3\gamma}^\dagger t_{4\gamma}] \cos(k_1 - k_3). \quad (14)$$

Finally, as in a standard spin-wave analysis, we perform a Bogoliubov transform

$$t_{k\alpha} = c_k \tau_{k\alpha} + s_k \tau_{-k\alpha}^\dagger, \quad (15)$$

where  $c_k = \cosh \theta_k$ ,  $s_k = \sinh \theta_k$ ,  $\theta_{-k} = \theta_k$ , which preserves the boson commutation relations

$$[\tau_{k\alpha}, \tau_{k'\beta}^\dagger] = \delta_{kk'} \delta_{\alpha\beta} \quad (16)$$

and is intended to diagonalize the Hamiltonian up to quadratic terms. After normal ordering, the transformed Hamiltonian up to fourth order terms reads

$$H = W_0 + H_2 + H_3 + H_4. \quad (17)$$

Here the constant term is

$$W_0 = 3N \left[ -\frac{1}{4} + R_2 - \frac{\lambda}{2} (R_3 + R_4) (1 - 8R_2 - 2R_1 + R_3 - R_4) \right] \quad (18)$$

expressed in terms of the momentum sums

$$R_1 = \frac{1}{N} \sum_k c_k s_k,$$

$$R_2 = \frac{1}{N} \sum_k s_k^2,$$

$$R_3 = \frac{1}{N} \sum_k c_k s_k \cos k,$$

$$R_4 = \frac{1}{N} \sum_k s_k^2 \cos k. \quad (19)$$

The quadratic terms are

$$H_2 = \sum_{k,\alpha} [E_k \tau_{k\alpha}^\dagger \tau_{k\alpha} + Q_k (\tau_{k\alpha} \tau_{-k\alpha} + \tau_{k\alpha}^\dagger \tau_{-k\alpha}^\dagger)] \quad (20)$$

where

$$E_k = (c_k^2 + s_k^2) \left[ 1 + 4\lambda (R_3 + R_4) - \frac{\lambda}{2} \cos k (1 - 2R_1 - 8R_2 - 2R_4) - \lambda c_k s_k [\cos k (1 - 8R_2 - 2R_1 + 2R_3) - 2(R_3 + R_4)] \right], \quad (21)$$

$$Q_k = c_k s_k \left[ 1 - \frac{\lambda}{2} [\cos k (1 - 2R_1 - 8R_2 - 2R_4) - 8(R_3 + R_4)] - \frac{\lambda}{4} (c_k^2 + s_k^2) [\cos k (1 - 8R_2 - 2R_1 + 2R_3) - 2(R_3 + R_4)] \right]. \quad (22)$$

The third- and fourth-order terms are

$$H_3 = \frac{\lambda}{2\sqrt{N}} \epsilon_{\alpha\beta\gamma} \sum_{123} [\delta_{1+2+3} \Phi_3^{(1)} (\tau_{1\alpha} \tau_{2\beta} \tau_{3\gamma} + \tau_{3\gamma}^\dagger \tau_{2\beta}^\dagger \tau_{1\alpha}^\dagger) + \delta_{1+2-3} \Phi_3^{(2)} (\tau_{1\alpha}^\dagger \tau_{2\beta}^\dagger \tau_{3\gamma} + \tau_{3\gamma}^\dagger \tau_{2\beta}^\dagger \tau_{1\alpha}^\dagger)] \quad (23)$$

and

$$H_4 = \frac{\lambda}{4N} \sum_{1234} [\delta_{1+2+3+4} \Phi_4^{(1)} (\tau_{1\alpha}^\dagger \tau_{2\alpha}^\dagger \tau_{3\gamma}^\dagger \tau_{4\gamma}^\dagger + \tau_{1\alpha} \tau_{2\alpha} \tau_{3\gamma} \tau_{4\gamma}) + \delta_{1+2-3-4} (\Phi_4^{(2)} \tau_{1\alpha}^\dagger \tau_{2\alpha}^\dagger \tau_{3\gamma} \tau_{4\gamma} + \Phi_4^{(3)} \tau_{1\alpha}^\dagger \tau_{2\gamma}^\dagger \tau_{3\alpha} \tau_{4\gamma}) + \delta_{1+2+3-4} \Phi_4^{(4)} (\tau_{1\alpha}^\dagger \tau_{2\alpha}^\dagger \tau_{3\gamma}^\dagger \tau_{4\gamma} + \tau_{4\gamma}^\dagger \tau_{3\gamma}^\dagger \tau_{2\alpha} \tau_{1\alpha})], \quad (24)$$

where we have used the shorthand notation  $1 \cdots 4$  for momenta  $k_1 \cdots k_4$ , and the vertex functions  $\Phi_3^{(i)}, \Phi_4^{(i)}$  are listed in Appendix A.

The condition that the off-diagonal quadratic terms vanish is

$$Q_k = 0. \quad (25)$$

In a conventional spin-wave approach, this would be implemented in leading order only, giving the condition

$$\tanh 2\theta_k = \frac{2c_k s_k}{c_k^2 + s_k^2} = \frac{\lambda \cos k}{2[1 - \lambda/2 \cos k]}. \quad (26)$$

This would leave some residual off-diagonal quadratic terms, arising from the normal-ordering of quartic operators. In a ‘‘modified’’ approach,<sup>16</sup> we demand that these terms vanish entirely up to the order calculated, giving the modified condition

$$\tanh 2\theta_k = \frac{\lambda[\cos k(1 - 8R_2 - 2R_1 + 2R_3) - 2(R_3 + R_4)]}{2[1 - \lambda \cos k(1 - 2R_1 - 8R_2 - 2R_4)/2 + 4\lambda(R_3 + R_4)]}. \quad (27)$$

Self-consistent solutions for the  $N$  equations (27), with the four parameters  $R_1 \cdots R_4$  given by Eq. (19), can easily be found by numerical means, starting from the conventional result (26).

### III. EXPANSION IN POWERS OF $\lambda$

As a first check on the formalism, one may calculate the leading terms in an expansion of the energy eigenvalues in powers of  $\lambda$ . From Eq. (26), we easily see that to order  $\lambda^2$

$$s_k = \frac{\lambda}{4} \cos k + \frac{\lambda^2}{8} \cos^2 k, \quad (28)$$

$$c_k = 1 + \frac{\lambda^2}{32} \cos^2 k, \quad (28)$$

and hence the lattice sums (19) can be evaluated

$$R_1 = \frac{\lambda^2}{16}, \quad R_2 = \frac{\lambda^2}{32}, \quad (29)$$

$$R_3 = \frac{\lambda}{8} + O(\lambda^3), \quad R_4 = O(\lambda^3). \quad (29)$$

The leading-order behavior of the vertex functions may easily be deduced from Appendix A.

Substituting in Eq. (18), the ground state energy per site is

$$\epsilon_0 = \frac{W_0}{2N} = \frac{3}{2} \left[ -\frac{1}{4} + R_2 - \frac{\lambda}{2}(R_3 + R_4) \right. \\ \left. \times (1 - 8R_2 - 2R_1 + R_3 - R_4) \right] \\ \sim -\frac{3}{8} - \frac{3\lambda^2}{64} - \frac{3\lambda^3}{256} + O(\lambda^4), \quad \lambda \rightarrow 0 \quad (30)$$

in agreement with dimer series expansion results previously obtained for this model.<sup>24</sup> One can easily show that perturbation diagrams such as those in Fig. 2 do not contribute until  $O(\lambda^4)$  or higher.

The energy gap at leading order can be found from Eq. (21):

$$E_k \sim 1 - \frac{\lambda}{2} \cos k + \frac{\lambda^2}{8} [4 - \cos^2 k], \quad \lambda \rightarrow 0. \quad (31)$$

The perturbation diagrams Figs. 3(a) and 3(b) also contribute at order  $\lambda^2$ . Note that diagram 3(b) does not appear in the formalism of Shevchenko *et al.*;<sup>14</sup> the extra terms in our formalism are needed to implement the hardcore constraint that two triplons cannot occupy the same site. At leading order, the contributions of these diagrams are

$$\Delta E_k^{3(a)} \sim -\frac{\lambda^2}{4} (1 + \cos k), \quad \lambda \rightarrow 0 \quad (32)$$

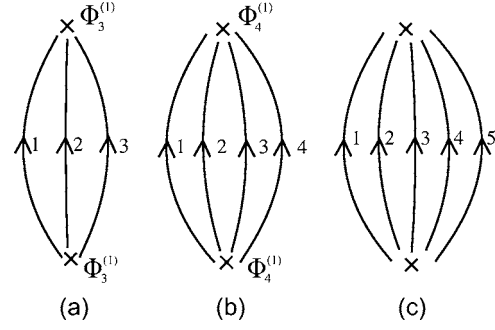


FIG. 2. Perturbation diagrams contributing to the ground-state energy.

$$\Delta E_k^{3(b)} \sim -\frac{\lambda^2}{4}, \quad \lambda \rightarrow 0 \quad (33)$$

(see the next section for further details). This gives a total single-particle energy

$$\epsilon_k \sim 1 - \frac{\lambda}{2} \cos k - \frac{\lambda^2}{8} \cos k [2 + \cos k], \quad \lambda \rightarrow 0 \quad (34)$$

which again agrees with series expansion results.<sup>24</sup>

If we compare Eq. (34) at small momentum with the continuum dispersion relation for a free boson,

$$\epsilon_k \sim \sqrt{m^2 c^4 + k^2 c^2}, \quad (35)$$

we readily discover the leading behavior of the effective triplon parameters, i.e., the triplon mass

$$m \sim \frac{2}{\lambda} [1 + \lambda + O(\lambda^2)] \quad (36)$$

and the “speed of light”

$$c \sim \frac{\lambda}{2} - \frac{3\lambda^2}{8} + O(\lambda^3) \quad (37)$$

in lattice units. Note that the mass diverges and the speed of light vanishes as  $\lambda \rightarrow 0$ .

### IV. NUMERICAL RESULTS

Writing the Hamiltonian as

$$H = H_0 + V \quad (38)$$

where

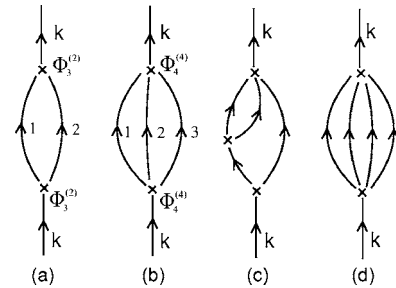


FIG. 3. Perturbation diagrams contributing to the one-particle energy.

$$H_0 = W_0 + H_2 \quad (39)$$

and

$$V = H_3 + H_4 \quad (40)$$

we can treat  $H_0$  as the unperturbed Hamiltonian and  $V$  as a perturbation to obtain the leading-order corrections to the predictions for physical quantities outlined in the previous section. Numerical results for the model have been obtained using the finite-lattice method. The momentum sums are carried out for a fixed number of dimers  $N$ , using corresponding discrete values for the momentum  $k$ , e.g.,

$$k_n = \frac{2\pi n}{N}, \quad n = 1, \dots, N. \quad (41)$$

Results were obtained for  $N$  up to 40, and a fit in powers of  $1/N$  was made to extrapolate to the bulk limit  $N \rightarrow \infty$ .

### A. Ground-state energy

The leading corrections to the ground-state energy correspond to the diagrams in Figs. 2(a) and 2(b). Their contributions are

$$\Delta \epsilon_0^{2(a)} = \frac{-9\lambda^2}{2N^2} \sum_{123} \delta_{1+2+3} \frac{\Phi_3^{(1)}(123)\Phi_3^{(1)}(123)}{(E_1 + E_2 + E_3)}, \quad (42)$$

$$\begin{aligned} \Delta \epsilon_0^{2(b)} &= \frac{-3\lambda^2}{4N^3} \sum_{1234} \delta_{1+2+3+4} \frac{\Phi_4^{(1)}(1234)}{(E_1 + E_2 + E_3 + E_4)} \\ &\times [3\Phi_4^{(1)}(1234) + \Phi_4^{(1)}(1324) + \Phi_4^{(1)}(1423)]. \end{aligned} \quad (43)$$

In leading order one can show that these terms are  $O(\lambda^4)$ , whereas diagrams such as Fig. 2(c) are  $O(\lambda^5)$  or higher. The resulting bulk estimates of the ground-state energy, including these corrections, are listed in Table I. Figure 4 shows the behavior of the ground-state energy as a function of  $\lambda$  resulting from this modified triplon theory, as compared with the high-order dimer series calculations of Zheng *et al.*<sup>24</sup> and exact diagonalization data of Barnes *et al.*<sup>19</sup> It can be seen that out to  $\lambda \approx 0.4$  there is quantitative agreement between our calculation and the series estimates, but some discrepancy emerges at larger  $\lambda$ .

### B. One-particle spectrum

The leading corrections to the one-particle spectrum correspond to the diagrams in Figs. 3(a) and 3(b). Their contributions are

$$\Delta E_k^{3(a)} = \frac{\lambda^2}{N} \sum_{12} \delta_{1+2-k} \frac{\Phi_3^{(2)}(12k)\Phi_3^{(2)}(12k)}{(E_k - E_1 - E_2)}, \quad (44)$$

$$\begin{aligned} \Delta E_k^{3(b)} &= \frac{\lambda^2}{8N^2} \sum_{123} \delta_{1+2+3-k} \frac{\Phi_4^{(4)}(123k)}{(E_k - E_1 - E_2 - E_3)} \\ &\times [3\Phi_4^{(4)}(123k) + \Phi_4^{(4)}(321k) + \Phi_4^{(4)}(312k)]. \end{aligned} \quad (45)$$

In leading order, these terms are  $O(\lambda^2)$ , as stated in the pre-

TABLE I. Values for the energy per dimer  $\epsilon_0$  and the energy gap at  $k=0$  as functions of  $\lambda$ . The left-hand side gives series estimates (Ref. 24) while the right-hand side gives our present triplet-wave results.

$\lambda$	Series expansion		Triplet expansion	
	$\epsilon_0$	Energy gap	$\epsilon_0$	Energy gap
0.0	-0.75000	1.00000	-0.75000	1.00000
0.1	-0.75096	0.94628	-0.75096	0.94647
0.2	-0.75394	0.88521	-0.75392	0.88625
0.3	-0.75914	0.81684	-0.75896	0.81885
0.4	-0.76672	0.74106	-0.76611	0.74252
0.5	-0.77694	0.65748	-0.77535	0.65483
0.6	-0.79010	0.56530	-0.78659	0.55341
0.7	-0.80662	0.46300	-0.79970	0.43649
0.8	-0.82712	0.34753	-0.81455	0.30312
0.9	-0.85268	0.21130	-0.83096	0.15309
1.0	-0.88630	0.00828	-0.84878	-0.01323

vious section, while diagrams like Figs. 3(c) and 3(d) are  $O(\lambda^3)$  or higher.

The resulting bulk estimates of the energy gap at  $k=0$  are listed in Table I and displayed in Fig. 5. It can be seen that the inclusion of Figs. 3(a) and 3(b) improves the agreement with series dramatically. This agreement may be fortuitous, given that the agreement for the ground-state energy is not so good, but it is gratifying to see nevertheless. It can be seen that our present approach improves upon that of Shevchenko *et al.*<sup>14</sup> at intermediate  $\lambda$ .

The dispersion of the one-particle energy as a function of momentum is illustrated at selected couplings in Fig. 6, while Figs. 7(a) and 7(b) show the corresponding behavior of the inverse triplon mass parameter  $1/m$  and the speed of light squared,  $c^2$ . At the smaller coupling, the dispersion agrees quantitatively with series estimates, but at  $\lambda=0.8$  we can see that the minimum of the energy is too broad: the

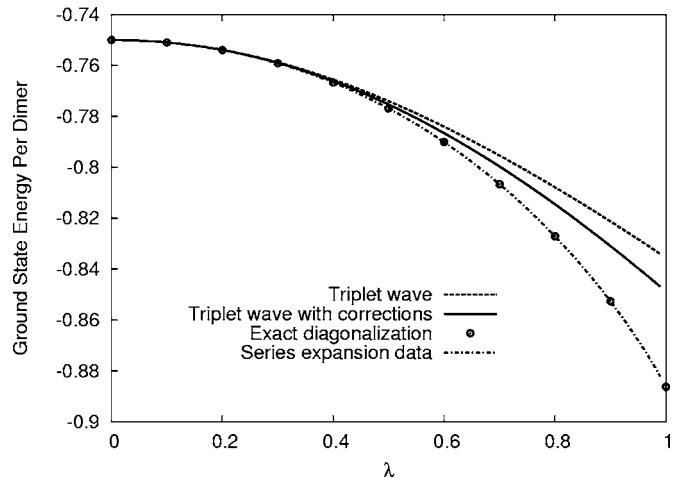


FIG. 4. Ground-state energy as a function of  $\lambda$ .

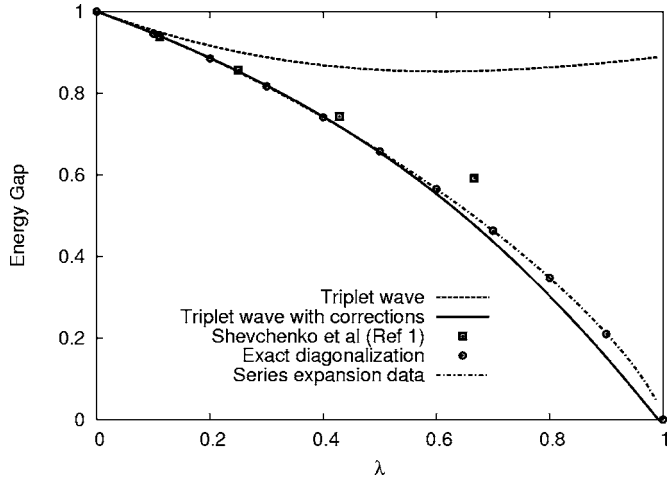


FIG. 5. Energy gap at  $k=0$  as a function of  $\lambda$ . The dot-dashed line shows the series estimates (Ref. 24), while the other lines show the leading order and improved triplet-wave results. The filled squares are results from Shevchenko *et al.* (Ref. 14), and circles are results from Barnes *et al.* (Ref. 19).

curvature at  $k=0$  should diverge as  $\lambda \rightarrow 1$ . This is reflected in the fact that our results for  $1/m$  and  $c^2$  are much too low at large couplings. We note that the exact value of the speed of light  $c$  at  $\lambda=1$  is  $\pi/2=1.57$ ,<sup>27</sup> which is about twice the value of even the series estimate ( $\approx 0.78$ ). This is presumably due to the singular behavior of the model in this limit, including logarithmic corrections, which even high-order series expansions cannot accurately reproduce.

### C. Two-triplon bound states

It has been found in previous studies<sup>14,20</sup> that the quartic terms in the Hamiltonian lead to attraction between two elementary triplons, giving rise to  $S=0$  and  $S=1$  bound states. We look for solutions of the two-body Schrödinger equation

$$H|\psi\rangle = E|\psi\rangle. \quad (46)$$

The two-body wave functions  $|\psi(K)\rangle$  can be written as follows:

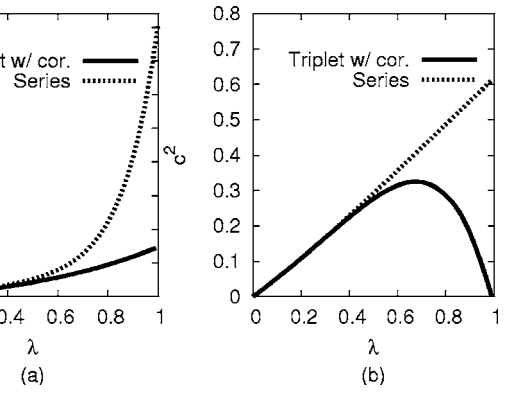
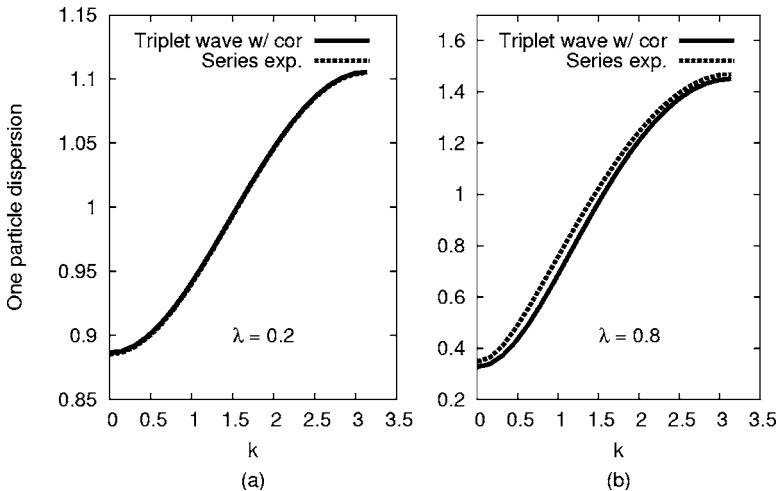


FIG. 7. (a) The inverse triplon mass parameter  $1/m$ , and (b) the “speed of light”  $c^2$ , as functions of  $\lambda$ .

*Singlet sector* ( $S=0$ ):

$$|\psi^S(K)\rangle = \frac{1}{\sqrt{6}} \sum_{q,\alpha} \psi^S(K,q) \tau_{K/2+q,\alpha}^\dagger \tau_{K/2-q,\alpha}^\dagger |0\rangle, \quad (47)$$

where  $K$  is the center-of-mass momentum and  $q$  the relative momentum of the two particles.

*Triplet sector* ( $S=1$ ):

$$|\psi_\alpha^T(K)\rangle = \frac{1}{2} \sum_{q,\beta,\gamma} \epsilon_{\alpha\beta\gamma} \psi^T(K,q) \tau_{K/2+q,\beta}^\dagger \tau_{K/2-q,\gamma}^\dagger |0\rangle, \quad (48)$$

where  $K$  is the center-of-mass momentum and  $q$  the relative momentum (we will not write out the quintuplet states explicitly).

From Eq. (46) one can readily derive the integral Bethe-Salpeter equation satisfied by the bound-state wave functions:

$$\begin{aligned} & [E^{S,T}(K) - E_{K/2+q} - E_{K/2-q}] \psi^{S,T}(K,q) \\ &= \frac{1}{N} \sum_p M^{S,T}(K,q,p) \psi^{S,T}(K,p). \end{aligned} \quad (49)$$

FIG. 6. One-particle spectrum at selected couplings.

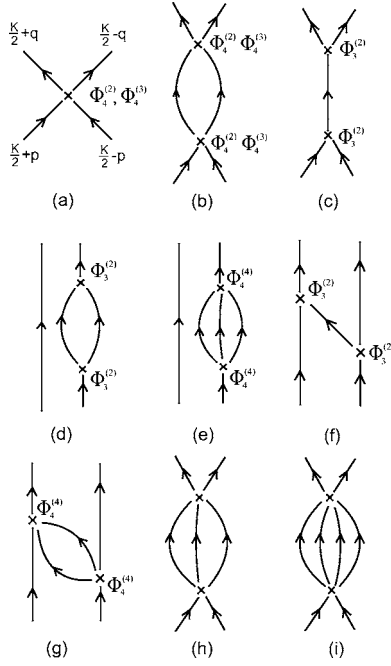


FIG. 8. Perturbation diagrams contributing to the two-particle scattering amplitude.

In leading order, the scattering amplitudes  $M^{S,T}(K, q, p)$  are simply given by the four-particle vertex from the perturbation operator  $V$ , Fig. 8(a). Hence we find for the different sectors:

*Singlet sector* ( $S=0$ ):

$$M^S(K, q, p) = \frac{\lambda}{2} [3\Phi_4^{(2)}(K/2 + p, K/2 - p, K/2 + q, K/2 - q) + \Phi_4^{(3)+}(K/2 + p, K/2 - p, K/2 + q, K/2 - q)], \quad (50)$$

where the wave function is symmetric,

$$\psi^S(K, -q) = \psi^S(K, q) \quad (51)$$

and the symmetric and antisymmetric pieces of the vertex function  $\Phi_4^{(3)}$  are defined:

$$\Phi_4^{(3)\pm} \equiv \frac{1}{2} [\Phi_4^{(3)}(1234) \pm \Phi_4^{(3)}(1243)]. \quad (52)$$

*Triplet sector* ( $S=1$ ):

$$M^T(K, q, p) = \frac{\lambda}{2} \Phi_4^{(3)-}(K/2 + p, K/2 - p, K/2 + q, K/2 - q) \quad (53)$$

with the wave function antisymmetric

$$\psi^T(K, -q) = -\psi^T(K, q). \quad (54)$$

*Quintuplet sector* ( $S=2$ ):

$$M^Q(K, q, p) = \frac{\lambda}{2} \Phi_4^{(3)+}(K/2 + q, K/2 - q, K/2 + p, K/2 - p), \quad (55)$$

where the wave function is once again symmetric

$$\psi^Q(K, -q) = \psi^Q(K, q). \quad (56)$$

At leading order in  $\lambda$ , we find

$$M^S(K, q, p) \sim \lambda [\cos(K/2)(\cos p + \cos q) - \cos p \cos q] \quad (57)$$

and

$$M^T(K, q, p) \sim -\frac{\lambda}{2} \sin p \sin q. \quad (58)$$

Following Shevchenko *et al.*,<sup>14</sup> one can then find simple solutions (unnormalized) to the Schrödinger equation (49):

$$\psi^S(K, q) \sim \frac{\cos(K/2) - \cos q}{1 + \cos^2(K/2) - 2 \cos(K/2) \cos q},$$

$$\psi^T(K, q) \sim \frac{\sin q}{1 + 4 \cos^2(K/2) - 4 \cos(K/2) \cos q}, \quad (59)$$

corresponding to bound-state energies

$$E^S(K) \sim 2 - \frac{\lambda}{2} [1 + \cos^2(K/2)],$$

$$E^T(K) \sim 2 - \frac{\lambda}{4} [1 + 4 \cos^2(K/2)] \quad (60)$$

compared to the lower edge of the two-particle continuum

$$E_2(K) \sim 2 - \lambda \cos(K/2). \quad (61)$$

These agree with the dimer series expansion<sup>19,25</sup> at leading order.

Note, however, that the singlet solution is valid for all  $K$ , touching the continuum at  $K=0$ ; while the triplet solution is only physically valid over a finite range of momenta  $K = \{2\pi/3, 4\pi/3\}$ , and not at  $K=0$ . The end points of this range are just where the triplet bound state enters the continuum, and the denominator of Eq. (59) for  $\psi^T$  vanishes at  $q=0$ . Note also that both dispersion curves meet the lower edge of the continuum at a tangent.

At the next order  $O(\lambda^2)$ , further diagrams contribute, as given in Figs. 8(b)–8(i). Two of these, Figs. 8(h) and 8(i), we are not in a position to calculate, because they involve five or six-particle vertices. Figure 8(b) is already accounted for by diagonalizing the effective Hamiltonian in the two-particle subspace. Figures 8(d) and 8(e) simply correspond to renormalizations of the single-particle energies in the diagonal terms of the effective Hamiltonian in the two-body sector. Finally, we can calculate the contribution of Figs. 8(c), 8(f), and 8(g) to the effective Hamiltonian using perturbation theory. In general, the change in the energy eigenvalue is

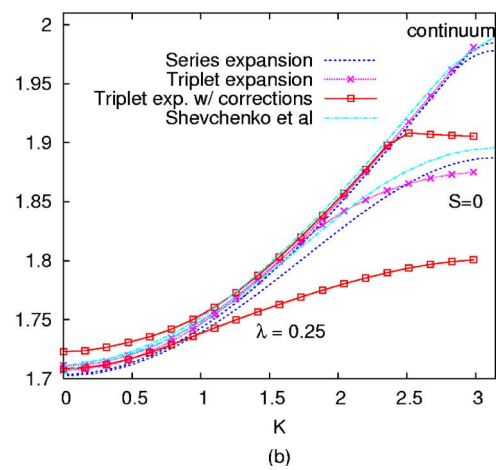
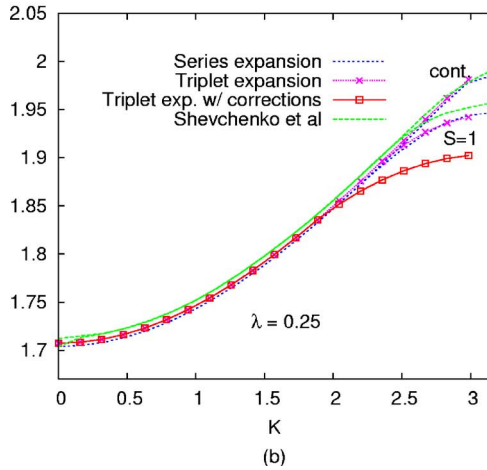
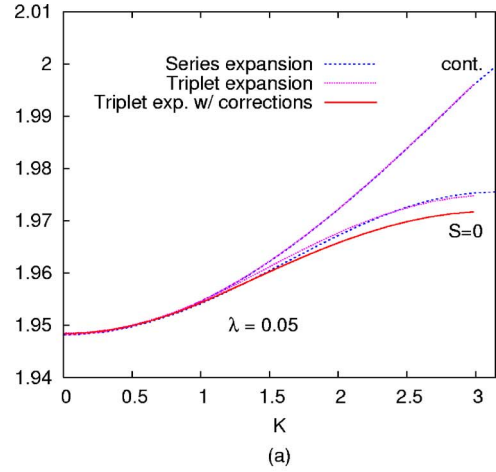
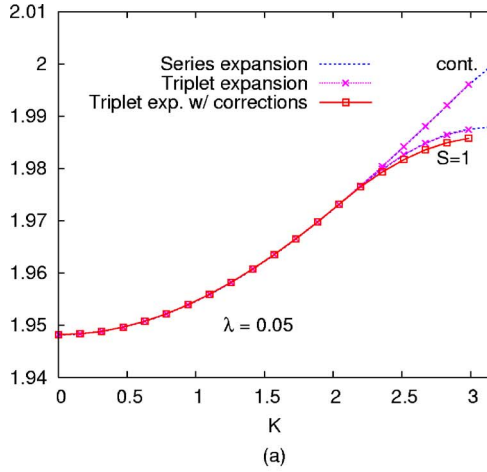


FIG. 9. (Color online) Dispersion relation for the triplet ( $S=1$ ) two-particle bound state at selected couplings (a)  $\lambda=0.05$  and (b)  $\lambda=0.25$ . The lower edge of the continuum is labeled “cont.”

$$\Delta E = \frac{1}{N} \sum_{p,q} \Delta M(K, q, p) \psi(K, p) \psi(K, q), \quad (62)$$

where the vertex function  $\Delta M(K, q, p)$  for each different diagram and spin state is listed in Appendix B.

The corrections due to these diagrams can now be calculated. On a finite lattice, Eq. (49) becomes a matrix eigenvalue equation, which can readily be solved numerically. We have calculated results for lattices of up to  $N=40$ . The resulting bound-state spectrum is displayed in Figs. 9 and 10. The first thing to note is that the modified but uncorrected triplet expansion agrees with series expansion estimates quite well, for both the lowest-lying singlet and triplet bound states. For the triplet state, the result is substantially better than that of Shevchenko *et al.*<sup>14</sup> at  $\lambda=0.25$ . Inclusion of the perturbation corrections actually makes the agreement worse, and gives much too large binding energies, especially at  $\lambda=0.25$ . This can be attributed to the neglect of Figs. 8(h) and 8(i), which are of the same order as the diagrams we have calculated. Unless the extra diagrams are included, we cannot do better than the uncorrected estimates.

We have also looked for signs of the second singlet and second triplet bound states which were found to appear at

FIG. 10. (Color online) Dispersion relation for singlet ( $S=0$ ) two-particle bound states at selected couplings (a)  $\lambda=0.05$  and (b)  $\lambda=0.25$ . The lower edge of the continuum is labeled “cont.”

order  $\lambda^2$  by Trebst *et al.*<sup>25</sup> In the corrected results, a second singlet bound state does appear, in fact, but with much too large a binding energy once again. The detailed dynamics of the bound states are sensitive to higher-order terms.

#### D. Structure factors

The “reduced exclusive structure factor” or spectral weight for a specific intermediate state  $\Lambda$  with momentum  $\mathbf{K}$  can be written

$$S_{\Lambda}^{\alpha\alpha}(K) = |\Omega_{\Lambda}^{\alpha}(K)|^2, \quad (63)$$

where

$$\Omega_{\Lambda}^{\alpha}(K) = \sqrt{N} \sum_{i^*} \langle \Psi_{\Lambda}(K) | S_{i^*}^{\alpha} | \Psi_0 \rangle \exp(-iKr_{i^*}) \quad (64)$$

and the sum  $i^*$  runs over sites of the unit cell on the lattice, and  $N$  is the number of unit cells (dimers). Using Eqs. (7), (13), and (15), the spin operators  $S_1$  and  $S_2$  on sites 1 and 2 can be expressed in terms of triplet operators [taking  $n=0$  in Eq. (13)]:

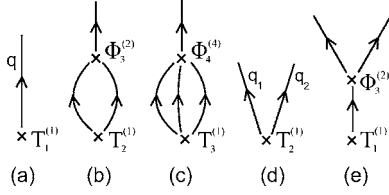


FIG. 11. Perturbation diagrams contributing to exclusive structure factors.

$$\begin{aligned}
 S_{1,2}^\alpha = & \pm \sum_k T_1^{(1)}(k)(\tau_{k\alpha} + \tau_{k\alpha}^\dagger) \\
 & - i\epsilon_{\alpha\beta\gamma} \sum_{12} [T_2^{(1)}(12)(\tau_{1\beta}^\dagger \tau_{2\gamma}^\dagger - \tau_{2\beta}^\dagger \tau_{1\gamma}^\dagger + \tau_{2\beta} \tau_{1\gamma} - \tau_{1\beta} \tau_{2\gamma}) \\
 & + T_2^{(2)}(12)(\tau_{1\beta}^\dagger \tau_{2\gamma} + \tau_{2\beta}^\dagger \tau_{1\gamma} - \tau_{2\gamma}^\dagger \tau_{1\beta} - \tau_{1\gamma}^\dagger \tau_{2\beta})] \\
 & \mp \sum_{123} [T_3^{(1)}(123)(\tau_{1\alpha}^\dagger \tau_{2\gamma}^\dagger \tau_{3\gamma}^\dagger + \tau_{2\gamma}^\dagger \tau_{3\gamma}^\dagger \tau_{1\alpha} + \tau_{1\alpha}^\dagger \tau_{2\gamma} \tau_{3\gamma} \\
 & + \tau_{2\gamma} \tau_{3\gamma} \tau_{1\alpha}) + T_3^{(2)}(123)(\tau_{1\alpha}^\dagger \tau_{2\gamma}^\dagger \tau_{3\gamma} + \tau_{3\gamma}^\dagger \tau_{2\gamma} \tau_{1\alpha})], \quad (65)
 \end{aligned}$$

where the upper and lower signs correspond to  $S_1^\alpha, S_2^\alpha$ , respectively, and

$$T_1^{(1)}(k) = \frac{1}{2\sqrt{N}}(c_k + s_k)(1 - R_1 - 4R_2), \quad (66)$$

$$T_2^{(1)}(12) = \frac{1}{8N}(c_1 s_2 - s_1 c_2), \quad (67)$$

$$T_2^{(2)}(12) = \frac{1}{8N}(c_1 c_2 - s_1 s_2), \quad (68)$$

$$T_3^{(1)}(123) = \frac{(c_1 + s_1)}{4N^{3/2}}(c_2 s_3 + s_2 c_3), \quad (69)$$

and

$$T_3^{(2)}(123) = \frac{(c_1 + s_1)}{2N^{3/2}}(c_2 c_3 + s_2 s_3). \quad (70)$$

In leading order [Fig. 11(a)], the one-particle matrix element is

$$\begin{aligned}
 \Omega_\Lambda^\alpha(K) = & i \sin\left(\frac{Ka}{2}\right) [(1 - R_1 - 4R_2)(c_K + s_K)] \\
 \sim & i \sin\left(\frac{Ka}{2}\right) \left[ 1 + \frac{\lambda}{4} \cos K + \frac{\lambda^2}{64} (5 \cos 2K - 7) \right]. \quad (71)
 \end{aligned}$$

Here  $a$  represents the spacing between spins in the dimer, i.e.,  $a=1/2$  for the uniform lattice in our present units.

Higher-order diagrams such as Figs. 11(b) and 11(c) do not contribute until  $O(\lambda^2)$ . Their contributions are listed in Appendix C. Hence we find

$$\Omega_{1p}^{\alpha(11b)} \sim i \cos\left(\frac{Ka}{2}\right) \frac{\lambda^2}{8} \sin K, \quad (72)$$

$$\Omega_{1p}^{\alpha(11c)} \sim i \sin\left(\frac{Ka}{2}\right) \frac{\lambda^2}{8}. \quad (73)$$

We must also account for the renormalization of the one-particle wave function due to Figs. 3(a) and 3(b), giving a multiplicative renormalization factor

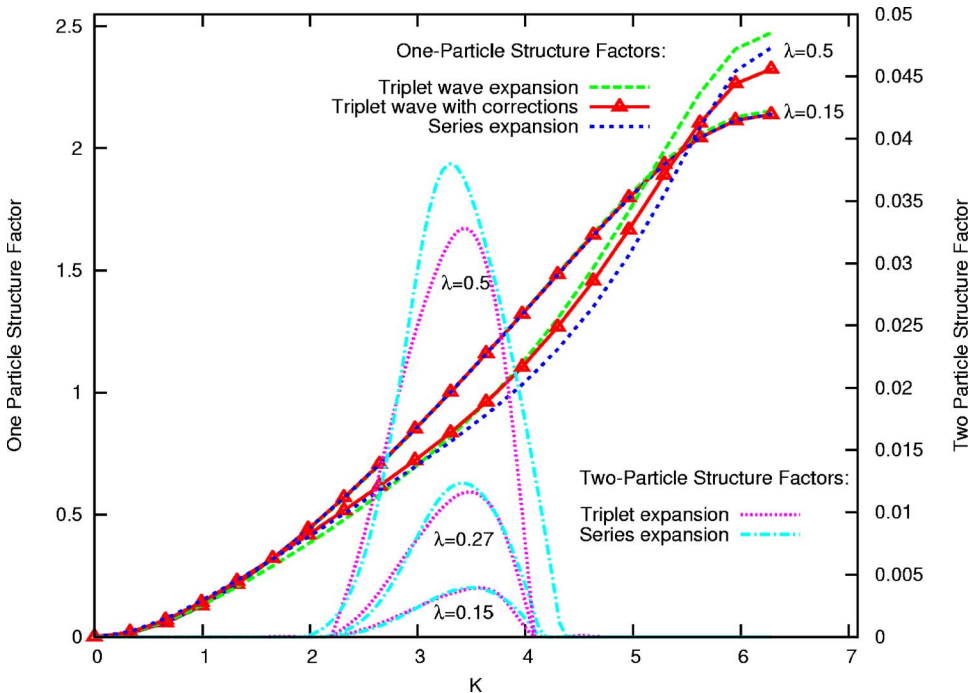


FIG. 12. (Color online) The one-particle (left axis) and two-particle (right axis) spectral weights as functions of momentum at selected couplings  $\lambda$ .

$$\begin{aligned}
Z_K &= 1 - \frac{\lambda^2}{2N} \sum_{12} \delta_{1+2-K} \left[ \frac{\Phi_3^{(2)}(12k)}{E_K - E_1 - E_2} \right]^2 \\
&\quad - \frac{\lambda^2}{16N^2} \sum_{123} \delta_{1+2+3-K} \frac{\Phi_4^{(4)}(123K)}{(E_K - E_1 - E_2 - E_3)^2} \\
&\quad \times [3\Phi_4^{(4)}(123K) + \Phi_4^{(4)}(321K) + \Phi_4^{(4)}(312K)] \\
&\sim 1 - \frac{\lambda^2}{8} \cos K - \frac{3\lambda^2}{16}
\end{aligned} \tag{74}$$

giving a total amplitude

$$\begin{aligned}
\Omega_{1p}^\alpha(K) &\sim i \left\{ \sin\left(\frac{Ka}{2}\right) \left[ 1 + \frac{\lambda}{4} \cos K \right. \right. \\
&\quad \left. \left. + \frac{\lambda^2}{64} (-11 - 8 \cos K + 5 \cos 2K) \right] \right. \\
&\quad \left. + \cos\left(\frac{Ka}{2}\right) \frac{\lambda^2}{8} \sin K \right\},
\end{aligned} \tag{75}$$

whereas Zheng *et al.*<sup>26</sup> obtain

$$\begin{aligned}
\Omega_{1p}^\alpha(K) &\sim i \left\{ \sin\left(\frac{Ka}{2}\right) \left[ 1 + \frac{\lambda}{4} \cos K \right. \right. \\
&\quad \left. \left. + \frac{\lambda^2}{6} (-11 - 4 \cos K + 5 \cos 2K) \right] \right. \\
&\quad \left. + \cos\left(\frac{Ka}{2}\right) \frac{\lambda^2}{8} \sin K \right\}.
\end{aligned} \tag{76}$$

We have been unable to resolve the source of the discrepancy at order  $\lambda^2$ .

The calculated results for the one-particle spectral weight are displayed in Fig. 12. It can be seen that the results match the series estimates quite well, even at larger  $\lambda$ . The corrected estimates are a little low at small  $k$ , and a little high at large  $k$ : this reflects the discrepancy at order  $\lambda^2$  referred to above.

For the two-particle bound states, the leading perturbation diagrams contributing to the exclusive structure factors are illustrated in Figs. 11(d) and 11(e). Their contributions for the triplet states are

$$\begin{aligned}
\Omega_T^{\alpha[11(d)]}(K) &= -8i\sqrt{N} \cos\left(\frac{Ka}{2}\right) \\
&\quad \times \sum_q \psi^T(K, q) T_2^{(1)}(K/2 + q, K/2 - q) \\
&\sim -i \frac{\lambda}{2\sqrt{N}} \cos\left(\frac{Ka}{2}\right) \sin(K/2) \\
&\quad \times \sum_q \sin q \psi^T(K, q)
\end{aligned} \tag{77}$$

and

$$\begin{aligned}
\Omega_T^{\alpha[11(e)]}(K) &= 2i\lambda \sin\left(\frac{Ka}{2}\right) T_1^{(1)}(K) \\
&\quad \times \sum_q \psi^T(K, q) \frac{\Phi_3^{(2)}(K/2 + q, K/2 - q, K)}{E_{K/2+q} + E_{K/2-q} - E_K} \\
&\sim i \frac{\lambda}{\sqrt{N}} \sin\left(\frac{Ka}{2}\right) \cos(K/2) \times \sum_q \sin q \psi^T(K, q).
\end{aligned} \tag{78}$$

Inserting the wave function (59), we obtain the leading order behavior of the triplet bound state contribution to the structure factor (for the uniform case  $a=1/2$ ):

$$S_T^{\alpha\alpha}(K) \sim \frac{\lambda^2}{2} \sin^6(K/4) [1 - 4 \cos^2(K/2)], \tag{79}$$

which agrees with the leading order series calculation.<sup>26</sup> Thus the bound-state spectral weight vanishes at the threshold points  $\{\cos(K/2) = \pm 1/2\}$  where the bound state merges with the continuum.

The numerically calculated results for the spectral weights are displayed in Fig. 12. For the one-particle weight, it can be seen that the corrected triplet-wave expansion matches the series estimates very well at the two lower couplings, and only begins to deviate significantly at  $\lambda=0.5$ . The triplet wave expansion also works surprisingly well for the two-particle weight, which is only of order 1% of the one-particle weight.

## V. SUMMARY AND CONCLUSIONS

In this paper, we have developed a modified triplet-wave expansion method for dimerized spin systems, analogous to the modified spin-wave formalism<sup>15,16</sup> for magnetically ordered systems. It differs from the earlier approaches of Sachdev and Bhatt<sup>7</sup> and Kotov *et al.*<sup>10</sup> in that projection operators are used to confine the system to the physical subspace in the bosonic formulation, eliminating the need for a separate constraint. The two-body boson operators are also fully diagonalized through the highest order calculated.

The formalism has been applied to the case of the alternating Heisenberg spin chain. Using perturbation theory to second order, we have calculated the ground-state energy per dimer, the dispersion relations for one-particle states and two-particle bound states, and the spectral weights for these states. It has been shown that the results reproduce the leading order terms in a dimer series expansion in powers of  $\lambda$ ,<sup>24-26</sup> apart from an unexplained discrepancy at order  $\lambda^2$  in the one-particle spectral weight. The results are quantitatively accurate at small  $\lambda$ , but begin to show significant discrepancies from high-order series expansions at larger  $\lambda$ , as one would expect. The discrepancies become more serious for the more sensitive dynamical quantities such as two-particle binding energies. The inclusion of a partial set of higher-order corrections for the two-particle binding energies made things worse rather than better, as one perhaps should have expected: all terms of a similar order in  $\lambda$  must be included simultaneously if a good result is to be obtained.

Nevertheless, the qualitative behavior is correctly reproduced by the formalism. In particular, the formation of two-triplon bound states near  $K=\pi/2$  in both the singlet ( $S=0$ ) and triplet ( $S=1$ ) channels, which were discovered previously,<sup>14,20</sup> is reproduced.

The behavior of the triplet bound state near the threshold where it merges with the continuum is interesting. We have seen that the bound-state dispersion curve merges at a tangent to the continuum, and that the spectral weight vanishes at the threshold. The bound-state solution does not extend into the continuum, but terminates at the threshold. This provides a neat example of the phenomenon of “quasiparticle breakdown” discussed recently in the literature:<sup>28–30</sup> i.e., the termination of a single-particle state where it enters the continuum for one-dimensional systems.

Our results appear to be more accurate and reliable at intermediate couplings  $\lambda$  than those of Shevchenko *et al.*<sup>14</sup> However, they cannot match the quantitative accuracy of the high-order dimer series expansions<sup>24–26</sup> or exact diagonalization on large lattices.<sup>19</sup> The calculations could be pushed to higher orders with the aid of a computer, but it is doubtful whether this is worthwhile. The main value of a “lattice bosonization” approach such as this is to provide a better analytic understanding of the behavior of the model, and a half-way house towards a continuum “effective field theory” for the model. For instance, we have shown how the triplon mass parameter and the “speed of light” can be calculated, which would be fundamental parameters of the effective field theory. It would be interesting to apply the approach to dimerized models in two dimensions.

### ACKNOWLEDGMENTS

We would like to thank J. Oitmaa and O. Sushkov for very useful discussions and advice. This work forms part of a research project supported by a grant from the Australian Research Council.

### APPENDIX A

The vertex functions  $\Phi_3^{(i)}, \Phi_4^{(i)}$  are

$$\Phi_3^{(1)}(123) = \frac{1}{6}[\sin k_1(c_1 + s_1)(c_2s_3 - s_2c_3) + \sin k_2(c_2 + s_2)(c_3s_1 - s_3c_1) + \sin k_3(c_3 + s_3)(c_1s_2 - s_1c_2)], \quad (\text{A1})$$

$$\Phi_3^{(2)}(123) = \frac{1}{2}[\sin k_1(c_1 + s_1)(c_2c_3 - s_2s_3) + \sin k_2(c_2 + s_2)(s_1s_3 - c_1c_3) + \sin k_3(c_3 + s_3)(s_1c_2 - c_1s_2)], \quad (\text{A2})$$

$$\begin{aligned} \Phi_4^{(1)}(1234) = & \frac{1}{4}[(\cos k_1 + \cos k_2)(c_1c_2 + c_1s_2 + s_1c_2 + s_1s_2)(c_3s_4 + s_3c_4) + (\cos k_3 + \cos k_4)(c_3c_4 + c_3s_4 + s_3c_4 + s_3s_4)(c_1s_2 + s_1c_2) \\ & + \cos(k_1 + k_4)(c_1s_4 - s_1c_4)(s_2c_3 - c_2s_3) + \cos(k_1 + k_3)(c_1s_3 - s_1c_3)(s_2c_4 - c_2s_4)], \end{aligned} \quad (\text{A3})$$

$$\begin{aligned} \Phi_4^{(2)}(1234) = & \frac{1}{2}[(\cos k_1 + \cos k_2)(c_1c_2 + c_1s_2 + s_1c_2 + s_1s_2)(s_3c_4 + c_3s_4) + (\cos k_4 + \cos k_3)(c_1s_2 + s_1c_2)(c_3c_4 + c_3s_4 + s_3c_4 + s_3s_4) \\ & + \cos(k_1 - k_3)(s_1c_2s_3c_4 + c_1s_2c_3s_4 - c_1c_2c_3c_4 - s_1s_2s_3s_4) + \cos(k_1 - k_4)(c_1s_2s_3c_4 + s_1c_2c_3s_4 - c_1c_2c_3c_4 - s_1s_2s_3s_4)], \end{aligned} \quad (\text{A4})$$

$$\begin{aligned} \Phi_4^{(3)}(1234) = & \cos k_1((c_1c_2 + s_1c_2)(s_3c_4 + c_3c_4) + (c_1s_2 + s_1s_2)(s_3s_4 + c_3s_4)) + \cos k_2((c_1c_2 + c_1s_2)(c_3s_4 + c_3c_4) + (s_1c_2 + s_1s_2)(s_3s_4 \\ & + s_3c_4)) + \cos k_3((c_1s_2 + s_1s_2)(c_3s_4 + s_3s_4) + (s_1c_2 + c_1c_2)(s_3c_4 + c_3c_4)) + \cos k_4((s_1c_2 + s_1s_2)(s_3c_4 + s_3s_4) + (c_1s_2 \\ & + c_1c_2)(c_3s_4 + c_3c_4)) + \cos(k_1 - k_4)(c_1c_4 - s_1s_4)(c_2c_3 - s_2s_3) + \cos(k_1 + k_2)(c_1s_2 - s_1c_2)(c_3s_4 - s_3c_4), \end{aligned} \quad (\text{A5})$$

$$\begin{aligned} \Phi_4^{(4)}(1234) = & (\cos k_1 + \cos k_2)(c_1c_2 + s_1s_2 + c_1s_2 + s_1c_2)(c_3c_4 + s_3s_4) + (\cos k_3 + \cos k_4)(c_1s_2 + s_1c_2)(c_3s_4 + s_3c_4 + c_3c_4 + s_3s_4) \\ & + \cos(k_2 + k_3)(c_1s_2c_3c_4 + s_1c_2s_3s_4 - c_1c_2s_3c_4 - s_1s_2c_3s_4) + \cos(k_1 + k_3)(s_1c_2c_3c_4 + c_1s_2s_3s_4 - c_1c_2s_3c_4 - s_1s_2c_3s_4). \end{aligned} \quad (\text{A6})$$

We have “symmetrized” these expressions with respect to their indices, using momentum conservation.

### APPENDIX B

The two-body terms  $\Delta M(K, p, q)$  defined in Eq. (52) for Figs. 8(c), 8(f), and 8(g) are as follows (the energy denominators are “symmetrized” between initial and final states):

Scalar state

$$\Delta M_S^{(9c)}(K, q, p) = 0, \quad (\text{B1})$$

Let

$$T_S^{(9f)}(K, q, p) = \lambda^2 \left\{ \frac{\Phi_3^{(2)}(p-q, K/2+q, K/2+p) \Phi_3^{(2)}(K/2-p, p-q, K/2-q)}{[E_{p-q} + 1/2(E_{K/2+q} + E_{K/2-p} - E_{K/2+p} - E_{K/2-q})]} \right\}$$

then

$$\Delta M_S^{(9f)}(K, q, p) = T_S^{(9f)}(K, q, p) + T_S^{(9f)}(K, -q, p) + T_S^{(9f)}(K, q, -p) + T_S^{(9f)}(K, -q, -p), \quad (\text{B2})$$

Let

$$T_S^{(9g)}(K, q, p) = -\frac{\lambda^2}{16N} \sum_k \{ \Phi_4^{(4)}(p-q-k, k, K/2+q, K/2+p) [3\Phi_4^{(4)}(k, p-q-k, K/2-p, K/2-q) + \Phi_4^{(4)}(K/2-p, k, p-q-k, K/2-q) + \Phi_4^{(4)}(K/2-p, p-q-k, k, K/2-q)] + 2\Phi_4^{(4)}(K/2+q, p-q-k, k, K/2+p) [3\Phi_4^{(4)}(K/2-p, k, p-q-k, K/2-q) + \Phi_4^{(4)}(k, p-q-k, K/2-p, K/2-q) + \Phi_4^{(4)}(K/2-p, p-q-k, k, K/2-q)] \} / [E_k + E_{p-q-k} + 1/2(E_{K/2+q} + E_{K/2-p} - E_{K/2+p} - E_{K/2-q})]$$

then

$$\Delta M_S^{(9g)}(K, q, p) = T_S^{(9g)}(K, q, p) + T_S^{(9g)}(K, -q, p) + T_S^{(9g)}(K, q, -p) + T_S^{(9g)}(K, -q, -p). \quad (\text{B3})$$

Triplet state

$$\Delta M_T^{(9c)}(K, q, p) = \lambda^2 \frac{\Phi_3^{(2)}(K/2+p, K/2-p, K) \Phi_3^{(2)}(K/2+q, K/2-q, K)}{[E_K - 1/2(E_{K/2+q} + E_{K/2-q} + E_{K/2+p} + E_{K/2-p})]}, \quad (\text{B4})$$

Let

$$T_T^{(9f)}(K, q, p) = \frac{\lambda^2}{2} \left\{ \frac{\Phi_3^{(2)}(p-q, K/2+q, K/2+p) \Phi_3^{(2)}(K/2-p, p-q, K/2-q)}{[E_{p-q} + 1/2(E_{K/2+q} + E_{K/2-p} - E_{K/2+p} - E_{K/2-q})]} \right\}$$

then

$$\Delta M_T^{(9f)}(K, q, p) = T_T^{(9f)}(K, q, p) - T_T^{(9f)}(K, -q, p) - T_T^{(9f)}(K, q, -p) + T_T^{(9f)}(K, -q, -p) \quad (\text{B5})$$

Let

$$T_T^{(9g)}(K, q, p) = -\frac{\lambda^2}{16N} \sum_k \{ \Phi_4^{(4)}(p-q-k, k, K/2+q, K/2+p) [3\Phi_4^{(4)}(k, p-q-k, K/2-p, K/2-q) + \Phi_4^{(4)}(k, K/2-p, p-q-k, K/2-q) + \Phi_4^{(4)}(p-q-k, K/2-p, k, K/2-q)] + 2\Phi_4^{(4)}(p-q-k, K/2+q, k, K/2+p) \times [\Phi_4^{(4)}(k, p-q-k, K/2-p, K/2-q) - \Phi_4^{(4)}(p-q-k, K/2-p, k, K/2-q)] \} / [E_k + E_{p-q-k} + 1/2(E_{K/2+q} + E_{K/2-p} - E_{K/2+p} - E_{K/2-q})]$$

then

$$\Delta M_T^{(9g)}(K, q, p) = T_T^{(9g)}(K, q, p) - T_T^{(9g)}(K, -q, p) - T_T^{(9g)}(K, q, -p) + T_T^{(9g)}(K, -q, -p). \quad (\text{B6})$$

### APPENDIX C

Contributions to the one-particle matrix elements  $\Omega_\Lambda^\alpha(K)$  from the diagrams shown in Figs. 11(b) and 11(c) are

$$\Omega_{1p}^{\alpha[11b]}(K) = 4i\lambda \cos\left(\frac{Ka}{2}\right) \sum_{12} \delta_{1+2-K} \frac{T_2^{(1)}(12)}{E_K - E_1 - E_2} [\Phi_3^{(2)}(21K) - \Phi_3^{(2)}(12K)], \quad (\text{C1})$$

$$\Omega_{1p}^{\alpha[11c]}(K) = -i \frac{\lambda}{\sqrt{N}} \sin\left(\frac{Ka}{2}\right) \sum_{123} \delta_{1+2+3-K} \frac{T_3^{(1)}(123)}{E_K - E_1 - E_2 - E_3} [3\Phi_4^{(4)}(321K) + \Phi_4^{(4)}(312K) + \Phi_4^{(4)}(213K)]. \quad (\text{C2})$$

- <sup>1</sup>B. S. Shastry and B. Sutherland, *Physica B* **108**, 1069 (1981).
- <sup>2</sup>For a review, see C. Lhuillier and G. Misguich, *Lecture Notes in Physics* (Springer, Berlin, 2002), Vol. 595, pp. 161–190.
- <sup>3</sup>N. Read and S. Sachdev, *Phys. Rev. Lett.* **66**, 1773 (1991); **62**, 1694 (1989); G. Murthy and S. Sachdev, *Nucl. Phys. B* **344**, 557 (1990).
- <sup>4</sup>V. N. Kotov, J. Oitmaa, O. P. Sushkov, and Z. Weihong, *Phys. Rev. B* **60**, 14613 (1999); O. P. Sushkov, J. Oitmaa, and W-H. Weihong, *ibid.* **63**, 104420 (2001).
- <sup>5</sup>P. W. Anderson, *Science* **235**, 1196 (1987).
- <sup>6</sup>L. Capriotti and S. Sorella, *Phys. Rev. Lett.* **84**, 3173 (2000); L. Capriotti, F. Becca, A. Parola, and S. Sorella, *Phys. Rev. B* **67**, 212402 (2003).
- <sup>7</sup>S. Sachdev and R. N. Bhatt, *Phys. Rev. B* **41**, 9323 (1990).
- <sup>8</sup>A. V. Chubukov, *JETP Lett.* **49**, 129 (1989).
- <sup>9</sup>D. C. Mattis, *The Theory of Magnetism*, Vol. II, Vol. 55 of Springer Series in Solid-State Sciences (Springer-Verlag, Berlin, 1981).
- <sup>10</sup>V. N. Kotov, O. Sushkov, Zheng Weihong, and J. Oitmaa, *Phys. Rev. Lett.* **80**, 5790 (1998).
- <sup>11</sup>P. V. Shevchenko and O. P. Sushkov, *Phys. Rev. B* **59**, 8383 (1999).
- <sup>12</sup>O. P. Sushkov and V. N. Kotov, *Phys. Rev. Lett.* **81**, 1941 (1998).
- <sup>13</sup>V. N. Kotov, O. P. Sushkov, and R. Eder, *Phys. Rev. B* **59**, 6266 (1999).
- <sup>14</sup>P. V. Shevchenko and O. P. Sushkov, *Phys. Rev. B* **59**, 8383 (1999).
- <sup>15</sup>M. Takahashi, *Phys. Rev. Lett.* **58**, 168 (1987); *Phys. Rev. B* **40**, 2494 (1989).
- <sup>16</sup>I. G. Gochev, *Phys. Rev. B* **49**, 9594 (1994).
- <sup>17</sup>G. Xu, C. Broholm, D. H. Reich, and M. A. Adams, *Phys. Rev. Lett.* **84**, 4465 (2000).
- <sup>18</sup>D. A. Tennant, C. Broholm, D. H. Reich, S. E. Nagler, G. E. Granroth, T. Barnes, K. Damle, G. Xu, Y. Chen, and B. C. Sales, *Phys. Rev. B* **67**, 054414 (2003).
- <sup>19</sup>T. Barnes, J. Riera, and D. A. Tennant, *Phys. Rev. B* **59**, 11384 (1999).
- <sup>20</sup>G. S. Uhrig and H. J. Schulz, *Phys. Rev. B* **54**, R9624 (1996).
- <sup>21</sup>A. Fledderjohann and C. Gros, *Europhys. Lett.* **37**, 189 (1997).
- <sup>22</sup>G. Bouzerar, A. P. Kampf, and G. I. Japaridze, *Phys. Rev. B* **58**, 3117 (1998).
- <sup>23</sup>G. Bouzerar and S. Sil, *Int. J. Mod. Phys. A* **15**, 2821 (2001).
- <sup>24</sup>R. R. P. Singh and Zheng Weihong, *Phys. Rev. B* **59**, 9911 (1999).
- <sup>25</sup>S. Trebst, H. Monien, C. J. Hamer, W-H. Zheng, and R. R. P. Singh, *Phys. Rev. Lett.* **85**, 4373 (2000); W. Zheng, C. J. Hamer, R. R. P. Singh, S. Trebst, and H. Monien, *Phys. Rev. B* **63**, 144411 (2001).
- <sup>26</sup>W. Zheng, C. J. Hamer, and R. R. P. Singh, *Phys. Rev. Lett.* **91**, 037206 (2003); C. J. Hamer, W. Zheng, and R. R. P. Singh, *Phys. Rev. B* **68**, 214408 (2003).
- <sup>27</sup>J. D. Johnson, S. Krinsky, and B. M. McCoy, *Phys. Rev. A* **8**, 2526 (1973).
- <sup>28</sup>T. Masuda, A. Zheludev, H. Manaka, L-P. Regnault, J-H. Chung, and Y. Qiu, *Phys. Rev. Lett.* **96**, 047210 (2006).
- <sup>29</sup>M. B. Stone, I. A. Zalisnyak, T. Hong, C. L. Broholm, and D. H. Reich, *Nature (London)* **440**, 187 (2006).
- <sup>30</sup>M. E. Zhitomirsky, *Phys. Rev. B* **73**, 100404(R) (2006).